sciendo

Management Systems in Production Engineering

2024, Volume 32, Issue 1, pp. 80-86

Date of submission of the article to the Editor: 06/2023
Date of acceptance of the article by the Editor: 01/2024

DOI 10.2478/mspe-2024-0009

ANALYSIS OF THE POSSIBILITY OF MODELING GAS SEPARATORS USING COMPUTATIONAL FLUID DYNAMICS

Vasyl Mykhailiuk
Ivano-Frankivsk National Technical University of Oil and Gas

Michał Zasadzień
Silesian University of Technology

Mikhailo Liakh, Ruslan Deineha, Yurii Mosora, Oleh Faflei
Ivano-Frankivsk National Technical University of Oil and Gas

Abstract:
Today, gas-liquid separators are usually used for the purification of gas mixtures from droplet liquid, and there are many designs of which. However, in order to improve the efficiency of their work, increase throughput, reduce mass and dimensions, they are constantly being improved. Usually, developing a new or improving an existing separator design is a long-term and relatively expensive process. Today, computer programs that implement the finite element method make it possible to speed up and reduce the cost of designing both a gas separator and other equipment. FloEFD program is one of these programs. However, it is more convenient during design to use one computer program that allows you to build 3D models (CAD) and in the same program to use a module for simulating the movement of gas and liquid flows (CFD). Such a program is SolidWorks with the FlowSimulation application module. As for the physical processes that occur during the operation of gas separators, they are quite complex, since a multiphase gas flow with an existing liquid phase is simulated. In the article, simulation modeling of the C-2-1 separator was carried out and the values and distributions of velocities and pressures in its various cross-sections were determined. Special attention was paid to the following cross-sections of the separator: along the axis of its inlet pipe; in the middle is the spigot of the blade screw; on a block of blinds. The difference in pressure at the outlet and inlet of the separator was determined, which is 20267 Pa. Based on the simulation results obtained, recommendations are given for further research and optimization of the separator design. The main parameter that characterizes the degree of separation of liquid from gas in the separator is the efficiency factor, which depends on the design of the separator, thermobaric conditions, parameters of the technological scheme, composition and physical and chemical properties of the gas-liquid flow. As a result of simulated modeling of the separator, its efficiency coefficient was determined when it extracted droplet liquid from the gas-liquid mixture in its various fractions (from 0.01 to 0.1 mm). The efficiency factor is about 100%.

Key words: *gas-liquid separator, efficiency coefficient, FlowSimulation, simulated modeling*

INTRODUCTION

Gas-liquid separators are simple devices for removing droplets of liquid using centrifugal force, gravity, etc. The advantages of these devices are the low cost of their operation. Maintenance is simple because separators have no complicated elements and no moving parts. Separators are used in many branches of industry: food, mining, petroleum, etc. Today, the main task in improving these devices is to minimize the pressure drop, increase the efficiency of separation, increase their productivity, and reduce overall dimensions and weight.

The purpose of the work is to analyze the possibility of using computational hydrodynamics to study the gas-liquid separator.

LITERATURE REVIEW

Gas purification from liquid and solid impurities, separation of heterogeneous gas-liquid and three-phase mixtures are the most widespread processes in oil and gas production,

oil and gas processing, chemical and petrochemical, construction and other industries [1, 2, 3, 4, 5].

The paper [6, 7] analyzes the features of the separation process of the flow of a two-phase gas-liquid mixture, which is fed from the supply pipe to the separator. Drops of the liquid phase (condensate) are formed in the flow, starting from the source of entry to the very entrance to the separator. In order to evaluate the efficiency of the separator, it is necessary to know the volume content of the liquid phase, the average droplet radius and their size distribution. Along the path of gas movement from the source of supply to the separator, the pressure and temperature change continuously. During movement, the thermodynamic equilibrium of a two-phase multicomponent system is disturbed and the process of mass transfer between phases occurs.

Condensation leads to the formation of small droplets, the size of which changes due to condensation growth in conditions of supersaturation and coagulation, as well as grinding in the gas flow. As a result, a size distribution of drops is established in the inlet pipe before the separator, which is characterized by: the content of the liquid phase, the average diameter of the drop and the dispersion of the distribution.

If there is no pre-condensation device in front of the separator, then the gas flow with the established distribution enters the separator, in which the phases are separated. In this case, the main mechanisms of droplet formation in a turbulent gas flow are the processes of grinding and coagulation, which occur simultaneously [6, 8, 9].

The main parameter that characterizes the degree of separation of liquid from gas in the separator is the efficiency coefficient, which is equal to the ratio of the volume of the liquid phase Q_{OC}, which settles in the separator, to the volume of the liquid phase Q_{BX}, which is contained in the gas stream at the entrance to the separator:

$$\eta = \frac{Q_{OC}}{Q_{BX}}.$$

The efficiency coefficient η depends on the design of the separator, thermobaric conditions, parameters of the technological scheme, composition and physical and chemical properties of the gas-liquid flow [10, 11].

Until recently, the development of new designs of separation equipment was carried out on the basis of the practical experience of previous researchers, as well as using simplified mathematical models. Of course, this approach required significant physical and economic costs and very often did not give the desired result. In the modern conditions of the development of computer technology, it is impossible to imagine the solution of complex current problems without the use of software complexes that provide an opportunity to simulate work processes in the device, the study of which is an extremely time-consuming task in practice [12, 13, 14]. Extensive development during the development of separation equipment programs that implement CFD methods [15, 16]. One such program is the program module SolidWorks – Flow Simulation [17, 18].

The use of CFD methods to study the behavior of oil particles in a separator is investigated in the works [19, 20]. The study conducted in [19] confirms the accuracy of CFD tools and methods by comparing numerical results with experimental data. On the other hand, the authors in [20] mainly present various CFD studies of separators using the VOF method, concluding that the numerical approach has many advantages, as it is cost-effective and flexible with respect to design changes. In addition, using numerical results, optimization of the separation process leads to improved designs of separators capable of capturing liquid particles up to 10 micrometers in size [21]. In [18, 22, 23], the authors apply CFD tools to study flow through a separator with different inlet designs, concluding that CFD methods are an effective tool for performance evaluation and separator design optimization processes.

EXPERIMENTAL

Research methods

Flow Simulation allows to calculate two-phase flows as a motion of particles in a steady-state flow field where the influence of the particles on the fluid flow (including its temperature) is negligible.

Generally, in this case the particles mass flow rate should be lower than about 30% of the fluid mass flow rate. To simulate dilute two-phase flows, where flows of gases or liquids contaminated with particles, the Lagrangian approach is used.

The particles of a specified (liquid or solid) material and constant mass are assumed to be spherical. The particles trajectories are determined by numerical integration of the equation:

$$m_p \frac{d\vec{U}_p}{dt} = \frac{1}{8}\pi\mu d\mathrm{Re}\ C_D\left(\vec{U} - \vec{U}_p\right) - \frac{1}{6}\pi d^3 \nabla P + m_p\vec{g} \qquad (1)$$

m_p is the particle mass,

$\vec{U}_p$ is the particle velocity vector, d is the particle diameter,

C_D is the particle resistance coefficient,

$\vec{g}$ is the gravitational acceleration vector,

*R*e is the Reynolds number based on the particle diameter, the relative velocity, and freestream density and viscosity.

The particle resistance coefficient is calculated with Henderson's formula, derived for continuum and rarefied, subsonic and supersonic, laminar, transient, and turbulent flows over the particles, and taking into account the temperature difference between the fluid and the particle. The particles' rotation, their interaction with each other, Brown motion and additional forces are not taken into account.

For subsonic flow (M ≤ 1):

$$C_D^{\mathrm{sub}} = 24\left[\mathrm{Re} + S\left(4.33 + \frac{3.65-1.53\frac{T_p}{T}}{1+0.353\frac{T_p}{T}}\exp\left(-0.247\frac{Re}{S}\right)\right)\right]^{-1} + \\ + \exp\left(-\frac{0.5M}{\sqrt{Re}}\right)\left[\frac{4.5+0.38(0.03\mathrm{Re}+0.48\sqrt{\mathrm{Re}})}{1+0.03\mathrm{Re}+0.48\sqrt{\mathrm{Re}}} + 0.1\mathrm{M}^2 + 0.2\mathrm{M}^8\right] + \\ + \left[1 - \exp\left(-\frac{M}{Re}\right)\right]0.6S \qquad (2)$$

For supersonic flow (M ≥ 1.75):

$$C_D^{\mathrm{super}} = \frac{\frac{0.9+0.34}{M_\infty^2} + 1.86\left(\frac{M_\infty}{Re_\infty}\right)^{0.5}\left[2 + \frac{2}{S_\infty^2}\left(\frac{T_p}{T}\right)^{0.5} - \frac{1}{S_\infty^4}\right]}{1+1.86\left(\frac{M_\infty}{Re_\infty}\right)^{0.5}} \qquad (3)$$

For the flow regimes with Mach between 1 and 1.75, a linear interpolation is to be used:

$$C_D = C_D^{sub}(1, Re) + \frac{4}{3}(M_\infty - 1)\left[C_D^{\mathrm{super}}(1.75, Re) - C_D^{sub}(1, Re)\right] \qquad (4)$$

where:
$C_D^{sub}(1, Re)$ is the drag coefficient calculated using the correlation for subsonic flow with M = 1,
$C_D^{\text{super}}(1.75, Re)$ is the drag coefficient calculated using the correlation for supersonic flow with M = 1.75,
M is the Mach number based on the relative velocity between the particle and the fluid flow,
$S = M\sqrt{\gamma/2}$ is the molecular speed ratio,
γ is the specific heat ratio,
T is the fluid temperature in freestream,
T_p is the particle temperature, and subscript '∞' refers to freestream conditions.
Thermal energy equation for a particle is given by:

$$m_p C_p \frac{dT_p}{dt} = \pi d \cdot k \cdot Nu(T - T_p) \quad (5)$$

where:
C_p is the specific heat of particle,
T_p is the particle temperature,
k is the thermal conductivity of fluid,
Nu is the Nusselt number.
The particle/fluid heat transfer coefficient is calculated with the formula:

$$Nu = \frac{2+0.459\mathrm{Re}^{0.55}\ \mathrm{Pr}^{0.33}}{1+3.42\frac{M}{\mathrm{Re}\ \mathrm{Pr}}(2+0.459\mathrm{Re}^{0.55}\ \mathrm{Pr}^{0.33})} \quad (6)$$

If necessary, the gravity is taken into account. Since the particle mass is assumed constant, the particles cooled or heated by the surrounding fluid change their size.
The interaction of particles with the model surfaces is taken into account by specifying either full absorption of the particles (that is typical for liquid droplets impinging on surfaces at low or moderate velocities) or ideal or non-ideal reflection (that is typical for solid particles). The ideal reflection denotes that in the impinging plane defined by the particle velocity vector and the surface normal at the impingement point, the particle velocity component tangent to surface is conserved, whereas the particle velocity component normal to surface changes its sign. A non-ideal reflection is specified by the two particle velocity restitution (reflection) coefficients, e_n and e_τ, determining values of these particle velocity components after reflection $V_{2,n}$ and $V_{2\tau}$, as their ratio to the ones before the impingement $V_{1,n}$, and $V_{1\tau}$:

$$e_n = \frac{V_{2,n}}{V_{1,n}},\ e_\tau = \frac{V_{2,\tau}}{V_{1,\tau}} \quad (7)$$

As a result of particles impingement on a solid surface, the total erosion mass rate ($R_{\Sigma e}$) and the total accretion mass rate ($R_{\Sigma e}$) are determined as follows:

$$R_{\sum e} = \sum_{i=1}^{N} K_i \cdot V_{pi}^b \cdot f_{1i}(\alpha_{pi}) \cdot f_{2i}(d_{pi}) d\dot{m}_{pi} \quad (8)$$

$$R_{\sum e} = \sum_{i=1}^{N} M_{pi} \quad (9)$$

where:
N is the number of fractions of particles specified by user as injections in Flow Simulation (the user may specify several fractions of particles, also called injections, so that the particle properties at inlet, i.e., temperature, velocity, diameter, mass flow rate, and material, are constant within one fraction),
I is the fraction number,
M_{pi} is the mass impinging on the model walls in unit time for the i-th particle fraction,
K_i is the impingement erosion coefficient specified by user for the i-th particle fraction,
V_{pi} is the impingement velocity for the i-th particle fraction,
b is the user-specified velocity exponent (*b* = 2 is recommended),
f_{1i} (α_{pi}) is the user-specified dimensionless function of particle impingement angle α_{pi},
f_{2i} (d_{pi}) is the user-specified dimensionless function of particle diameter d_{pi}.

Simulation modeling

As mentioned above, gas-liquid separators are complex devices, the operation of which uses many different physical principles. This makes it difficult to simulate their work. In order to carry out high-quality simulation modeling, one should have a step-by-step methodology that would guarantee not only numerical convergence, but also enable further verification of the computational model from simple to complex cases.
Let's consider the methodology used. At the first stage of modeling, only the gas phase is taken into account (taking into account the composition of the gas). The modeling process itself is performed until the convergence of the results according to one or more selected criteria occurs. When the stability of the results of simulation modeling is achieved, it is necessary to proceed to the second stage of modeling. At this stage, the application module FlowSimulation "Particle Studies" is used. Here, the introduction of fine-drop liquid into the gas flow takes place, taking into account the size of its particles, their consumption, etc. It is with the help of this module that the separator efficiency coefficient is determined. To determine it, the number of liquid particles at the entrance to the separator and at the exit from it are compared.

3D separator model and finite volume mesh

For the research, a 3D model of the C-2-1 separator was built, which is shown in Figure 1.

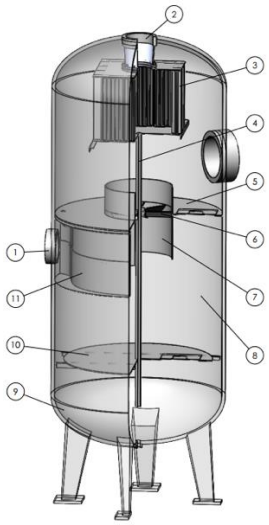

Fig. 1 3D model of the separator C-2-1:
1 – inlet pipe; 2 – outlet pipe; 3 – block of blinds; 4 – drain pipe; 5 – partition; 6 – blade screw; 7 – blade screw guide; 8 – housing; 9 – bottom; 10 – bumper; 11 – guide channel (deflector)

The structure and principle of operation of the separator are as follows: the gas-liquid mixture enters the inlet pipe 1, where the direction of its movement changes (from straight to circular) due to the guide channel (deflector) 11. Due to the action of centrifugal force, liquid droplets (large particles) are separated from the gas-liquid mixture. The separated liquid flows down the inner wall of the housing 8 and settles in the bottom 9. The gas-liquid mixture with small liquid particles moves up through the blade screw guide 7 and the blade screw 6 itself. With the help of a blade screw, the gas-liquid flow is swirled. Next, the gas-liquid mixture exits from the vane screw guide and its speed decreases and drops of liquid fall from the gas-liquid flow onto the partition 5, from which the liquid is diverted through the drain hole into the deflector 11. After that, the gas-liquid mixture enters the block of blinds, on which the smallest liquid particles settle. From the block of blinds, the separated liquid flows into the bottom 9 through the drain pipe 4, and the purified gas exits into the outlet pipe 1.

As for the main design parameters of the separator, its internal diameter is 1800 mm, the length of the cylindrical part of the body is 3390 mm, and the internal diameter of the inlet and outlet nozzles is 294 mm. The diameter of the blade screw is 720 mm. Regarding the dimensions of the block of blinds, the length of the walls is 906 mm, the thickness of the walls is 100 mm, and the height of the block is 712 mm. Purified gas from the block of blinds exits through a nozzle with a diameter of 273 mm.

As for the finite element mesh applied to the separator, it has certain features. In the FlowSimulation program, the following grid construction options are possible: global and local. It should be noted that there are small gaps in the design of the separator, and accordingly, when using a global grid, they will either not be taken into account, or the obtained results will not have sufficient accuracy. Therefore, for such elements, an individual approach is applied using a local grid with its appropriate settings. Figure 2 shows the finite element mesh, and Figure 3 shows the local finite element mesh in the cross section of the separator louver block.

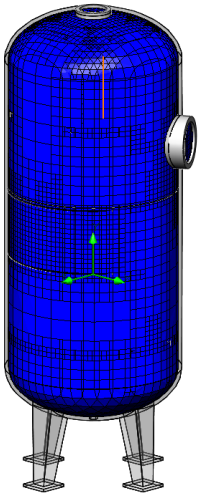

Fig. 2 Mesh of finite elements

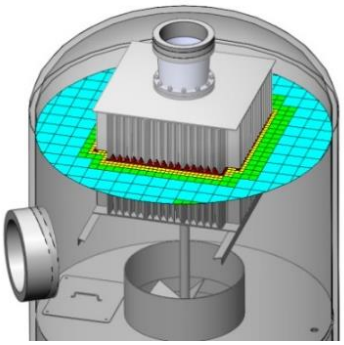

Fig. 3 Local mesh of finite elements in the cross section of the block of separator blinds

Boundary conditions and settings

The volume flow rate of the gas mixture is set at the inlet of the separator in the amount of 1.56 m^3/s (Fig. 4). The velocity on all walls of the separator is zero.

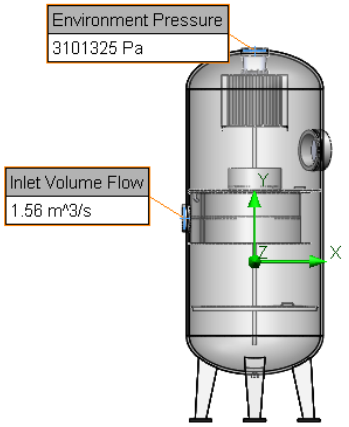

Fig. 4 Boundary conditions

A pressure of 3 MPa is set at the outlet of the separator. Such values of pressure and consumption of the gas mixture are determined by the technological scheme of gas separation at the production site where the studied separator is used.

Since the gas flow is multicomponent, that is, it consists of a mixture of different gases, their volume concentration is also taken into account during the simulation. The composition of the gas mixture: methane – 93%; hydrogen – 0.1%; ethane – 2.5%; propane – 0.31%; butane – 0.11%; methanol – 0.08%.

To control the parameters of the separator, several of its cross-sections were selected, which have the greatest effect on the efficiency of its operation (fig. 5). Such cross-sections include: cross-section of the separator along the axis of the inlet pipe (A-A); cross-section of the separator in the middle of the guide nozzle of the blade screw (B-B); cross-section of the separator in the middle of the height of the block of blinds (C-C).

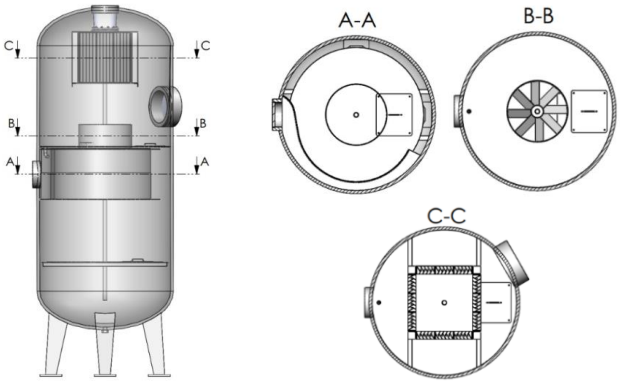

Fig. 5 Selection of separator cross-sections for parameter control

Since the main purpose of the separator under consideration is to clean the gas stream from liquid droplets, the "Particle Studies" module was used in the FlowSimulation program to determine the separation efficiency coefficient. In this module, the following fractions of liquid (water) drops are set: 0.01-0.1 mm with a step of 0.01 mm. Also, the direction of action of gravitational forces and flow rate of droplet liquid of 0.00783 kg/s are specified in the settings.

RESULTS

When deriving the results of simulating the operation of the separator, it should be noted that it is possible to consider two variants of the values of the controlled parameters: the global maximum and the local maximum. It is understood that when the results are displayed in the cross-section along the axis of the separator, when selecting the "global maximum" parameter, the maximum value of the controlled parameter can be located at another point (part) of the separator. Therefore, to control the parameters in the selected cross-sections of the separator, the "local maximum" parameter should be used, for which the maximum value of the parameter will be in the considered cross-section.

Figure 6 shows the distribution of pressure and velocity in the longitudinal section of the separator.

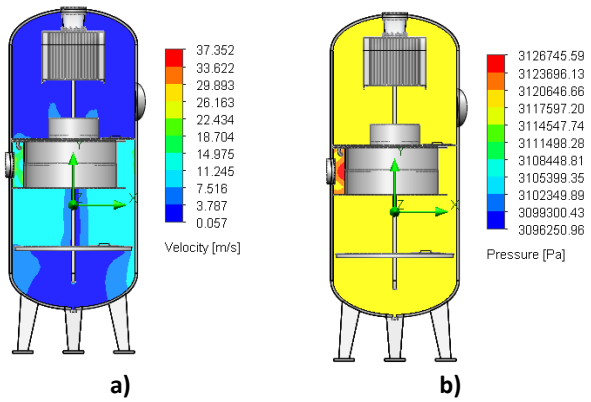

Fig. 6 Distribution of velocity (a) and pressure (b) in the longitudinal section of the separator

Below are the pressure and velocity distributions in the above sections of the separator (Fig. 7-9).

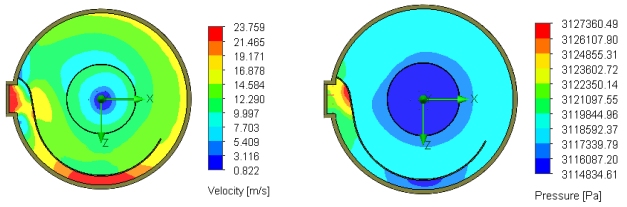

Fig. 7 Distribution of velocity (a) and pressure (b) and in the cross section of the separator along the axis of the inlet nozzle

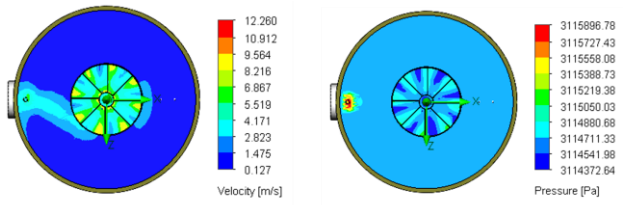

Fig. 8 Distribution of speed (a) and pressure (b) and in the cross section of the separator in the middle of the guide nozzle of the blade propeller

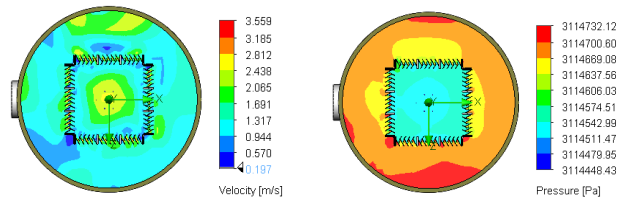

Fig. 9 Distribution of speed (a) and pressure (b) and in the cross section of the separator in the middle, the height of the block of blinds

Figure 10 shows the distribution of liquid fractions of 0.1 mm (a) and 0.01 mm (b) in the separator.

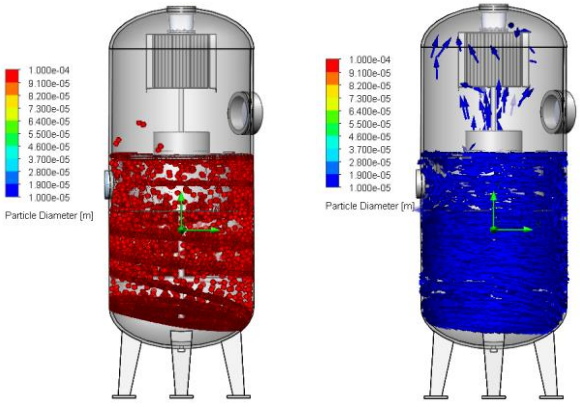

Fig. 10 Distribution of the liquid fraction of 0.1 mm (a) and 0.01 mm (b) in the separator

Since one of the main parameters of the separator is the pressure drop (resistance) created by us, we will determine its value and consider the zones of the separator that cause it. According to Figure 11, the pressure at the inlet to the separator is 3121592 Pa, and at the outlet is 3101325 Pa.

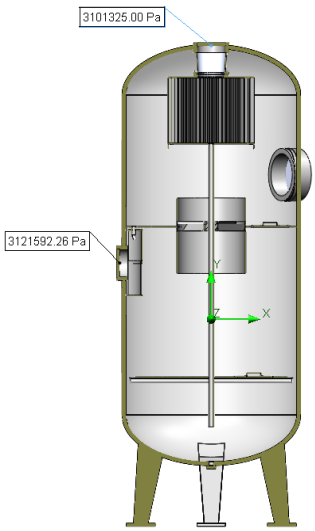

Fig. 11 Values of pressure at the inlet and outlet of the separator

It can be seen from Figure 6b that the main zone of the separator (if we consider the longitudinal section of the separator) in which the greatest pressure is created is the transition from the inlet pipe to the guide device (deflector). The occurrence of this resistance (increase in pressure) is due to the direct (radial) entry of the gas-liquid flow into the separator, during which the flow hits the wall of the guide apparatus and at the same time the speed of its movement decreases. This is clearly reflected in Figure 7b. To reduce the resistance created in the considered area of the separator, it is advisable to supply the gas-liquid mixture tangentially (tangentially) to the separator body.

Regarding the distribution of pressure and velocity of the gas-liquid flow in the cross-section of the separator in the middle of the height of the block of blinds (Fig. 9), there are zones where the speed of movement decreases to zero. In further work, it is expedient to carry out simulation simulations of the operation of the separator louver unit, to set their optimal dimensions according to the performance of the separator, to select the necessary geometric parameters (tilt angles, wall thickness, etc.).

As a result of simulated modeling of the behavior of a gas mixture with different fractions of water present in it, it was established that at a given flow rate of the gas-liquid mixture, the coefficient of efficiency of the separator is equal to almost 100%. That is, none of the water fractions is removed with the gas flow from the separator.

CONCLUSION

According to the results of the conducted simulation modeling of the gas-liquid separator, the value of the resistance created by it at the given input parameters: the flow at the inlet nozzle and the pressure at the outlet nozzle was determined. The resistance value is 20267 Pa.

The coefficient of efficiency of the separator when extracting droplet liquid of various fractions (from 0.01 to 0.1 mm) was established. The value of the coefficient of efficiency is about 100%.

In the following studies of the separator, in order to increase its productivity, reduce overall dimensions and weight, it is necessary to divide the separator into separate component elements and carry out simulation modeling with them. This will make it possible to optimize the designs of these elements by paying more attention to them and reduce the processor time for solving the problem.

REFERENCES

[1] V.V. Mykhailiuk, O.Ya. Faflei, V.O. Melnyk, I.Ya. Zakhara, A.R. Malyshev and H.Ya. Protsiuk, 2022. Modeling of a gas vertical grid separator. Scientific Bulletin of Ivano-Frankivsk National Technical University of Oil and Gas. 1(52), pp. 91-100. DOI:10.31471/1993-9965-2022-1(52)-91-100.

[2] L.M. Mil'shtein, Modernization of Oil and Gas Field Separation. Development of New-Generation Separation Units and Apparatuses, *LAP Press*, Saarbrücken, Germany (2012).

[3] C.S. Liu, 1994. Development and field test of separator in prying loading type gas collecting device. *Natural Gas and Petroleum.* 1236-40

[4] V. Vijayan, M. Vivekanandan, R. Venkatesh, et al. 2021. CFD modeling and analysis of a two-phase vapor separator. *J Therm Anal Calorim* 145, pp. 2719-27261. DOI:10.1007/s10973-020-09825-2

[5] J. Kou, Z. Li. Numerical Simulation of New Axial Flow Gas-Liquid Separator. Processes*. 2022; 10(1):64.* DOI:*10.3390/pr10010064*

[6] M.M. Liakh, E.V. Yuriev, V.M. Vakaliuk, Ya.V. Solonychnyi. 2008. Matematychna model separatsii hazoridynnoi sumishi v separatori inertsiinoho typu. *Rozvidka ta rozrobka naftovykh i hazovykh rodovyshch*. № 1. pp. 67-73.

[7] Ye, Junxiang & Xu, Yanxia & Song, Xingfu & Yu, Jianguo. 2019. Novel conical section design for ultra-fine particles classification by a hydrocyclone. Chemical Engineering Research and Design. 144, pp. 135-149, DOI:10.1016/j.cherd.2019.02.006.

[8] Caie Zhang, & Wei, Dezhou & Cui, Baoyu & Li, Tianshu & Na. Luo, 2017. Effects of curvature radius on separation behaviors of the hydrocyclone with a tangent-circle inlet. Powder Technology. 305, 156-165, DOI:10.1016/j.powtec.2016.10.002.

[9] E. Mahmoud & Zhou, Ling & Shi, Weidong & Chen, Han. 2021. Performance evaluation of standard cyclone separators by using CFD–DEM simulation with realistic bio-particulate matter. Powder Technology. 385, pp. 357-374, DOI:10.1016/j.powtec.2021.03.006.

[10] B. Wiencke. 2011. Fundamental principles for sizing and design of gravity separators forindustrial refrigeration. *International Journal of Refrigeration.* 34**,** pp. 2092-2108. DOI:10.1016/j.ijrefrig.2011.06.011.

[11] Chu, Kaiwei, B. Wang, D.L. Xu, Y.X. Chen, Aibing Yu. 2011. CFD-DEM simulation of the gas – solid flow in a cyclone separator. *Chemical Engineering Science*. 66. pp. 834-847. DOI:10.1016/j.ces.2010.11.026.

[12] K. Pravin, A. Krupan, A. Dewasthale, A. Datar, A.S. Dalkilic, 2021. CFD analysis of cyclone separator used for fine filtration in separation industry. *Case Studies in Thermal Engineering*. 28. 101384. DOI:10.1016/j.csite.2021.101384.

[13] Chu, Kaiwei, B. Wang, D.L. Xu, Y.X. Chen, Aibing Yu,. 2011. CFD–DEM simulation of the gas–solid flow in a cyclone separator. *Chemical Engineering Science*. 66. pp. 834-847. DOI:10.1016/j.ces.2010.11.026.

[14] O. Vytyaz, I. Chudyk, V. Mykhailiuk, 2015. Study of the effects of drilling string eccentricity in the borehole on the quality of its cleaning. New Developments in Mining Engineering 2015: *Theoretical and Practical Solutions of Mineral Resources Mining*. pp. 591-595.
[15] N.D. Katopodes, Free-Surface Flow: Computational Methods, Oxford, UK: Butterworth-Heinemann, 2019
[16] V. Dragan, I. Malael, B. Gherman, 2016. A Comparative Analysis Between Optimized and Baseline High Pressure Compressor Stages Using Tridimensional Computational Fluid Dynamics. *Engineering, Technology & Applied Science Research*, *6*(4), pp. 1103-1108. DOI: 10.48084/etasr.696.
[17] V.V, Maistruk R.I. Havryliv A.S.Popil, A.M. Basistyi 2012.Otsinka enerhozatrat pry roboti priamotechiinoho tsyklonu za dopomohoiu prohramnoho paketu FLOW SIMULATION. Vostochno-Evropeyskiy zhurnal peredovyih tehnologiy. 6/8(60). pp. 28-30.
[18] F.P. Lucas and R. Huebner, "Numerical Simulation of Single-Phase andTwo-Phase Flows in Separator Vessels with Inclined Half-Pipe InletDevice Applied in Reciprocating Compressors," Engineering, Technology & Applied Science Research, vol. 8, no. 3, pp. 2897-2900, Jun. 2018, https://doi.org/10.48084/etasr.1993.
[19] S.C.K. De Schepper, G.J. Heynderickx, and G.B. Marin. 2008. CFD modeling of all gas-liquid and vapor-liquid flow regimes predicted by the Baker chart," *Chemical Engineering Journal*. 138. 1. pp. 349-357, DOI: 10.1016/J.CEJ.2007.06.007.
[20] A.P. Laleh, W.Y. Svrcek, and W.D. Monnery. 2012. Design and CFD studies of multiphase separators – a review," *The Canadian Journal of Chemical Engineering*. 90. 6. pp. 1547-1561. DOI: 10.1002/CJCE.20665.
[21] G. Cheng, L. Yan, and H. Zhou, 2004. The Oil Vessel Structure Optimization by the use of CFD in the Oil Injection Twin-Screw Compressor," presented at the International Compressor Engineering Conference, West Lafayette, IN, USA, Art. no. 1714.
[22] Xu. Yanxia, Ye. Junxiang, Xingfu Song, Jianguo Yu. 2022. Classification of Ultrafine Particles Using a Novel 3D-Printed Hydrocyclone with an Arc Inlet: Experiment and CFD Modeling. ACS Omega. 8. DOI:10.1021/acsomega.2c06383.
[23] J.Y. Tian, L. Ni, T. Song, J.N. Zhao. 2020. CFD simulation of hydrocyclone – separation performance influenced by reflux device and different vortex – finder lengths. Sep. Purif. Technol. 233, No. 116013. DOI: 10.1016/j.seppur.2019.116013

Vasyl Mykhailiuk
ORCID ID: 0000-0002-3329-2068
Ivano-Frankivsk National Technical University
of Oil and Gas
15 Karpatska st., 76019 Ivano-Frankivsk, Ukraine
e-mail: myhajlyukv@ukr.net

Michał Zasadzień
ORCID ID: 0000-0002-3181-9815
Silesian University of Technology,
Roosevelta 26, 41-800 Zabrze, Poland
e-mail: michal.zasadzien@polsl.pl

Mikhailo Liakh
ORCID ID: 0000-0001-9447-6605
Ivano-Frankivsk National Technical University
of Oil and Gas
15 Karpatska st., 76019 Ivano-Frankivsk, Ukraine
e-mail: mm.lyakh@gmail.com

Ruslan Deineha
ORCID ID: 0000-0003-1141-7672
Ivano-Frankivsk National Technical University
of Oil and Gas
15 Karpatska st., 76019 Ivano-Frankivsk, Ukraine
e-mail: deynega2004@ukr.net

Yurii Mosora (correspondence author)
ORCID ID: 0000-0002-3192-7146
Ivano-Frankivsk National Technical University
of Oil and Gas
15 Karpatska st., 76019 Ivano-Frankivsk, Ukraine
e-mail: yuramosora@gmail.com

Oleh Faflei
ORCID ID: 0000-0002-6415-117X
Ivano-Frankivsk National Technical University
of Oil and Gas
15 Karpatska st., 76019 Ivano-Frankivsk, Ukraine
e-mail: olehfaflei@gmail.com